Group VIII Carbamoyl Complexes as Catalysts for Alkyne Hydrocarboxylation and Electrochemical Proton Reduction

Chandan Kr Barik, Malcolm E. Tessensohn, Richard D. Webster and Weng Kee Leong*

Division of Chemistry & Biological Chemistry, Nanyang Technological University, 21 Nanyang Link, Singapore, 637371.

Abstract: A series of group VIII carbamoyl complexes, [M(2-NHC(O)C_5H_4N)$(CO)_2$(2-SC_5H_4N)] [where M = Fe, Ru and Os], was found to be efficient and regioselective catalysts for the intramolecular hydroxycarboxylation of α,ω-alkynoic acids, yielding exocyclic enol lactones for ring sizes up to 7 atoms, and endocyclic enol lactones for ring sizes up to 12 atoms. They also catalysed the regioselective intermolecular hydroxycarboxylation reaction between propargylic alcohol and carboxylic acids to form β-oxo-esters. These complexes could also function as electrocatalysts in proton reduction, and evaluation of their redox potentials revealed that the iron complex was much more efficient than the ruthenium or osmium analogues.

Keywords: Group 8 metals; carbamoyl; catalysis; alkyne hydrocarboxylation; proton reduction

1. Introduction

The hydrogenases are naturally-occurring metalloenzymes which are involved in the utilization of hydrogen.[1,2,3] There are three classes of hydrogenases of which the [Fe]-hydrogenase has a simple metal cofactor which comprises a single iron centre.[4,5,6,7] There has been a lot of research focused on functional as well as structural mimics of this metal cofactor.[8,9,10,11] We recently reported the synthesis and physical properties of metallacyclic carbamoyl complexes **1n** as structural analogues of this cofactor for the group VIII triad, *viz*., iron, ruthenium and osmium (Figure 1b).[12,13,14] An interesting aspect of these complexes is that the 2-mercaptopyridine ligand is hemilabile; it imparts stability to the complexes and yet is capable of de-coordination at the pyridine-N.[12] This property makes the complexes potential catalysts and indeed, as we would like to report here, they are efficient catalysts for alkyne hydroxycarboxylation and electrochemical proton reduction.

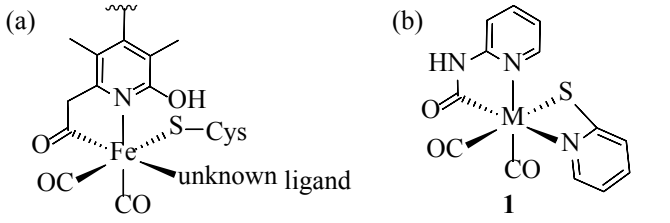

Figure 1. Structure of the (a) active site of [Fe]-hydrogenase, and (b) metallacyclic carbamoyl complexes **1n**.

2. Results and discussion

2.1. Alkyne hydrocarboxylation

The hydrocarboxylation of terminal alkynes can occur intramolecularly to afford enol lactones, or intermolecularly to β-oxo-esters (Scheme 1). Both these classes of products are important and useful. The enol lactones are present in many natural products with biological activity,[15,16,17] and may occur as an endocyclic ring,[18] or as an exocyclic substructure,[19] with the latter serving as useful

* Corresponding author.
E-mail address: chmlwk@ntu.edu.sg (W. K. Leong).

intermediates in the syntheses of more complex compounds such as parthenolide, helenalin and arglabin.[20,21,22] Similarly, the acetonyl ester motif of α,ω-oxo-esters can be found in several natural compounds and biologically active steroids.[23,24,25]

The cyclization of α,ω-alkynoic acids represents an effective synthetic approach to the enol lactones; the exocyclic and endocyclic products being obtained via Markovnikov and anti-Markovnikov addition, respectively.[15,26] A large number of metal-based catalysts have been reported for the intra- and intermolecular hydrocarboxylation of terminal alkynes - molybdenum,[27] ruthenium,[28,29,30,31] rhodium,[32] palladium,[33] platinum,[34] and gold.[35,36] Among these, only two ruthenium complexes, *viz*., [TpRu{PhCNC(Ph)CCPh)(PMe^{i}Pr$_2$}] and [TpRuH(PPh$_3$)$_2$], have been reported for the intramolecular reaction;[37] the former gives the endocyclic enol lactone and the latter a mixture of both the exocyclic and endocyclic enol lactones, but neither is selective for the exocyclic enol lactone.

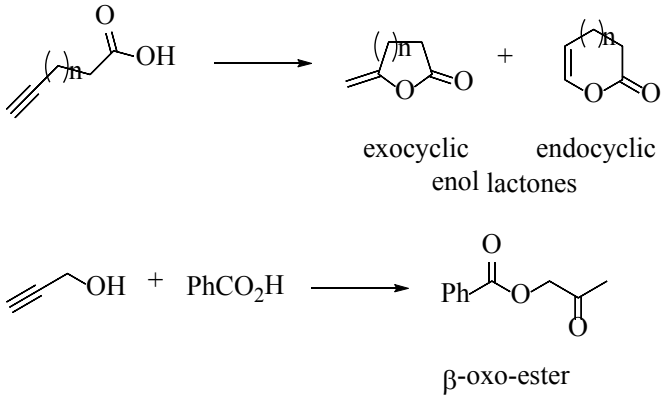

Scheme 1. Hydrocarboxylation reaction of terminal alkynes.

The complexes **1** catalyze the intramolecular hydrocarboxylation of a wide range of terminal alkynes (Table 1). The hydrocarboxylation of 5-hexynoic acid in the presence of **1b**, for example, gives the corresponding exocyclic enol lactone **2b**, regioselectively and exclusively via intramolecular nucleophilic attack of the acid. The cyclization takes place smoothly in refluxing toluene within 12 h and with 1.4% catalyst loading. Optimization of the catalyst loading for **1b** suggests an optimal loading of 1.4 mol-% (Table S1). The product obtained depends on the chain length of the alkynoic acid, HOOCCH$_2$(CH$_2$)$_n$CCH; the exocyclic enol lactone **2** is obtained for n = 1-3 (entries 2-4) whereas endocyclic enol lactone **3** results for n = 7 (entry 5), under the same reaction conditions; a control reaction without **1b** affords no product (entry 1). All the cyclization products are allowed under Baldwin's rules. Cyclization for the larger cyclic enol lactone is also not stereoselective, giving a mixture of both the *Z*- and *E*-enol lactones. The yield also appears to decrease with an increase in the ring size, and may be ascribed to the higher thermodynamic stability of the smaller rings. An attempt at the cyclization of 5-hexynoic acid with **1a** fails due to catalyst decomposition at higher temperature, and **1c** shows similar catalytic efficiency and selectivity to that of **1b** (entries 6 and 7).

Table 1. Intramolecular hydrocarboxylation of terminal alkynes.

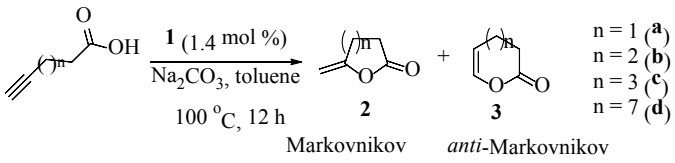

Entry	Catalyst	n	Product ratio **2n**:**3n**	Yield (%)[a]	Turnover Number
1	**1a**	1	0	0	0
2	**1b**	1	100:0	93	71
3	**1b**	2	100:0	98	75
4	**1b**	3	100:0	57	44
5	**1b**	7	0:100[b]	80	61
6	**1c**	1	100:0	62	47
7	**1c**	2	100:0	77	59
8	**1c**	7	0:100[b]	68	52

[a]NMR yields with anisole as internal standard. [b]A 55:45 mixture of *Z*/*E* isomers, determined by integration of the ^{1}H NMR spectrum.

Complex **1b** is also a good catalyst for the intermolecular hydrocarboxylation of propargyl

alcohol, giving the β-oxo-ester regioselectively; complex **1c** shows similar activity. The molecular structure of one of the products, **4d**, has been confirmed crystallographically (Table S4). In the absence of the alcohol functionality, regioselectivity is lost and all three possible products, with the *E* product as the major species, is obtained; this is illustrated for the reaction with *p*-ethynyltoluene (Table 2).

Table 2. Intermolecular hydrocarboxylation of terminal alkynes.

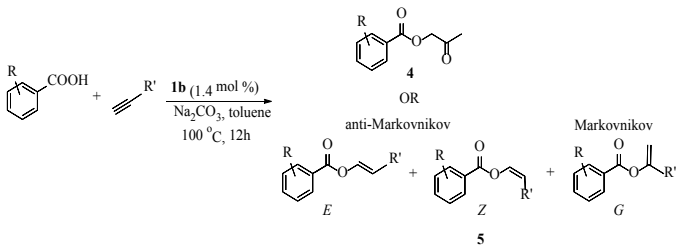

Entry	R	R'	Product, % (*E:Z:G*)[a]	Turnover Number
1	H	CH_2OH	**4a**, 90	69
2	*o*-Me	CH_2OH	**4b**, 88	68
3	*o*-OMe	CH_2OH	**4c**, 90	69
4	*p*-CH_2Br	CH_2OH	**4d**, 84	64
5	*p*-Br	CH_2OH	**4e**, 80	61
6	H	*p*-tolyl	**5a**, 92 (55:28:17)	70
7	*o*-Me	*p*-tolyl	**5b**, 90 (5:3:2)	69

[a]NMR yields with anisole as internal standard. Ratio of the products obtained by integration of the ^{1}H NMR spectrum.

The catalytic pathway is presumably similar to those previously suggested; the proposed pathway for the intramoleular alkyne hydrocarboxylation is shown in Scheme 2.[28,32] We have already established that the carbamoyl ligand exerts a very strong trans effect and hence it will labilize decoordination of the nitrogen atom of the 2-mercaptopyridine ligand in **1n**.[22] The resulting complex **A** allows for coordination of the alkyne moiety to **B**, and intramolecular nucleophilic attack by the carboxylate group at the *α*- or β-position (to **C** and **C**, respectively), followed by protonolysis, would afford either the Markovnikov (exocyclic) or anti-Markovnikov (endocyclic) product, respectively. An attempt to identify a species corresponding to intermediate **B** was carried out via a reaction between **1b** and propargyl alcohol but no such species was observable. The change in selectivity with the chain length may have to do with steric factors; with a shorter chain, the *α*-position is more accessible, and formation of a terminal alkenyl complex is also favoured, while this is decreased for a longer chain length. The intermolecular hydrocarboxylation probably follows a similar pathway, favouring attack by the carboxylate group at the *α*-position of the metal-bound alkyne.

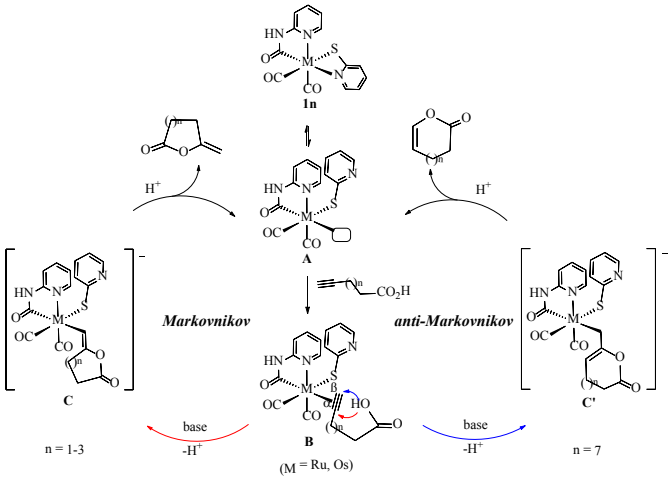

Scheme 2. Proposed catalytic cycle for the alkyne hydrocarboxylation.

2.2. Electrocatalytic proton reduction

A recent report on two complexes which are structurally similar to **1n**, *viz*., [Fe(2-$CH_2C(O)C_5H_3NCH_2OCOR)(CO)_2$(2-$SC_5H_3N$)] where R = Me (**6a**) or Ph (**6b**), as potential electrocatalysts for proton reduction prompted us to assess the complexes **1n** for a similar function.[38] The cyclic voltammograms (CV) of **1a-c** display chemically irreversible oxidation and reduction waves (measured in acetonitrile, scan rate of 0.1 V s^{-1}) which are similar to those reported for **6a** and **6b** (Figure S1). As may be expected, the first oxidation

potential increased in the order **1a**(Fe) < **1b**(Ru) < **1c**(Os) (+0.75, +0.77 and +0.83 V versus Fc/Fc^+, respectively), and the potential for **1a** is slightly more positive than those reported for **6a** and **6b** (0.60 and 0.68 V versus Fc/Fc^+, respectively). The small differences in the potentials for **1a-c** suggest that this first oxidation is ligand- rather than metal-centred, based on comparisons against the CVs of the free ligands 2-aminopyridine and 2-mercaptopyridine (Figure S3). Consistent with this, a DFT study carried out on **1b** shows that the HOMO resides mostly on the sulphur atom (see supplementary information).

A similar trend is observed for the first reduction potential, which increased (became more negative) in the order **1a**(Fe) < **1b**(Ru) < **1c**(Os) (-1.90, -2.22 and -2.27 V versus Fc/Fc^+, respectively); the larger differences suggest metal-centred reduction, although the computed LUMO is essentially ligand-centred. The oxidation and reduction processes were found to be independent of each other, although additional oxidation processes (that were not observed when the initial direction was towards positive potentials) were noted on the reverse scan when the initial direction was swept towards negative potentials. A CPE experiment on **1b** suggests that the same number of electrons are transferred for both the oxidation and reduction waves.[39]

The cathodic current increased with the amount of trifluoroacetic acid (TFA) added; that for **1a** is shown in Figure 2, and this behavior is consistent with catalytic proton reduction.[40,41] This was verified with a combination of CPE and GC experiments. A TOF of 2.4 h^{-1} was measured for **1a** at a constant potential of -2.11 V (versus Fc/Fc^+ couple) over a period of 30 min. The estimated current produced at a fixed over-potential (-0.21 V versus Fc/Fc^+ couple) was much higher than that for the other two complexes (Figure S2), thus indicating that **1a** is much more efficient, and can be attributed to its lower first reduction potential.[42,43]

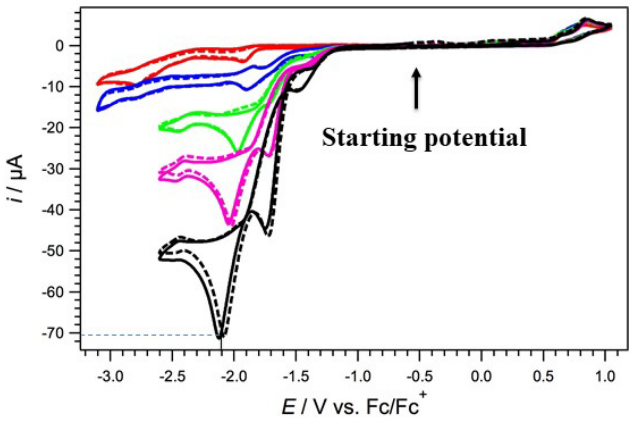

Figure 2. Cyclic voltammogram of **1a** (1.0 mM)/ *n*-Bu_4NPF_6 (0.1 M) in CH_3CN and TFA at 0 (red), 2 (blue), 5 (green), 10 (pink) and 20 (black) mM. Scan rate = 0.1 V s^{-1}, T = 25±2 °C with the starting potential at -0.6 V vs. Fc/Fc^+. Solid and dashed lines represent initial scans towards the positive and negative directions, respectively.

Crossover of the forward and reverse scans may indicate some deposition on the surface but this was observed only at higher concentrations of TFA. Although the mechanism for the electrocatalytic proton reduction has not been studied in detail, it is probably similar to that reported for the other hydrogenase model complexes; a simplified pathway is depicted in Scheme 3. It is likely that initial protonation and reduction occurs at the S atom and the hydrogen is subsequently transferred to the metal centre.[42,43,44]

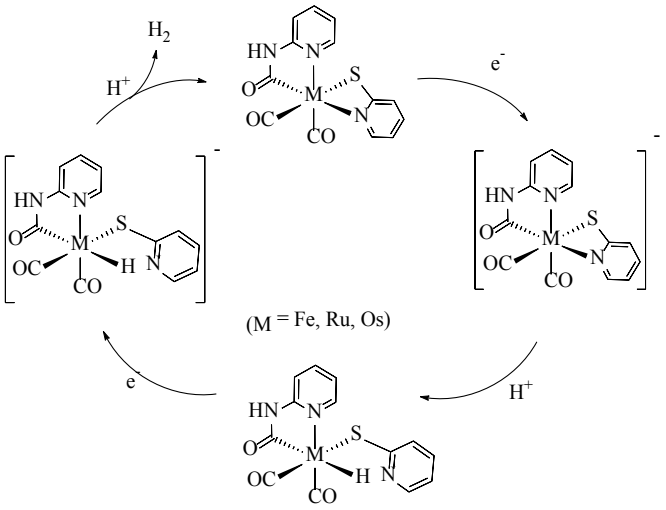

Scheme 3. Proposed mechanism for the electrocatalytic proton reduction.

3. Conclusion

We have shown in this work that the group VIII metal complexes [M(2-NHC(O)C_5H_3NR)$(CO)_2$(2-SC_5H_4N)] (where M = Fe, Ru or Os) are good and selective catalysts for the intra- and intermolecular hydroxycarboxylation of terminal akynes, as well as electrocatalysts for proton reduction. While the iron complex was found to be the most efficient in proton reduction, it was unstable under the conditions for alkyne hydrocarboxylation and, in that case, the ruthenium complex was much better.

4. Experimental

4.1. General procedures

All experiments were performed under an argon atmosphere using standard Schlenk techniques. Chemicals were obtained from Sigma Aldrich and used as received. The compounds **1n** were synthesized according to the literature procedure.[12] Solvents that were used for reactions were distilled over the appropriate drying agents under argon before use. TLC separations were carried out on 20 x 20 cm^2 plates coated with silica gel 60 F254 from Merck. HRMS were recorded in ESI mode on a Waters UPLC-Q-Tof MS mass spectrometer. ^{1}H NMR spectra were obtained on a JEOL 400 MHz spectrometer at room temperature, and the chemical shifts were referenced to the residual chloroform resonance. Electrochemical measurements were made using a computer-controlled Eco Chemie Autolab PGSTAT302N potentiostat in a three-electrode cell with a 1 mm diameter planar glassy carbon disk (Cypress Systems) working electrode, a platinum wire (Metrohm) auxiliary electrode, and a silver wire (Cypress Systems) miniature reference electrode connected to the main solution via a salt bridge containing 0.5 M n-Bu_4NPF_6 in CH_3CN. Gas chromatography measurements were made using Agilent 7890A gas-chromatograph with a thermal conductivity detector (TCD), a 5 Å molecular sieve column (2 mm × 5 m), and argon as the carrier gas.

4.2. Catalytic runs

In a typical run, the acid (0.78 mmol), propargyl alcohol (0.07 ml, 1.2 mmol), Na_2CO_3 (4 mg, 0.03 mmol) and the catalyst (1.4 mol %), were dissolved in toluene (10 ml) and stirred for 12 h at 100 °C. After cooling to room temperature, the mixture was filtered and the filtrate was then evaporated under a vacuum. The residue was then purified by thin layer chromatography to afford the product.

4.3. Electrochemical experiments

The electrolyte (0.1 M *n*-Bu_4NPF_6 in MeCN) was de-oxygenated by purging with high purity argon gas prior to each run. Working electrodes were cleaned by polishing with an alumina (grain size 0.3 μm) slurry on a Bueller Ultra-pad polishing cloth, rinsed with ultrapure water, acetone and then dried. All voltammetric experiments were performed at room temperature (25 ± 2 ºC) inside a Faraday cage; ferrocene was added as an internal reference to the solutions at the end of each measurement. Bulk controlled potential electrolysis (CPE) experiments were performed in a two-compartment CPE cell divided by a porosity 5 sintered glass frit.[39] Identically sized glassy carbon cylindrical rods (length 6 cm, outer diameter 1.8 cm and internal diameter 1.2 cm) were employed as the working and auxiliary electrodes and symmetrically arranged with respect to each other.

Acknowledgements

This work was supported by Nanyang Technological University and the Ministry of Education (Research Grant No. M4011793). C.K.B is grateful to the university for a Research Scholarship. We acknowledge the help of Drs Yongxin Li and Rakesh Ganguly with the crystallographic work.

Appendix A. Supplementary data

CCDC 1892017 contains the supplementary crystallographic data for **4d**. This is available from the Cambridge Crystallographic Data Centre. Spectroscopic data for all compounds, optimization of the catalytic reaction, details of the

crystallographic study, and CVs reported. This material is available free of charge via the Internet.

5. References

1. R. K. Thauer, A.-K. Kaster, M. Goenrich, M. Schick, T. Hiromoto, S. Shima, Annu. Rev. Biochem. 79 (2010) 507-536.
2. P. M. Vignais, Bioenergetics, Springer: 2007; 223-252.
3. T. Buhrke, O. Lenz, A. Porthun, B. Friedrich, Mol. Microbiol. 51 (2004) 1677-1689.
4. S. Shima, R. K. Thauer, Chem. Rec. 7 (2007) 37-46.
5. C. Zirngibl, R. Hedderich, R. Thauer, FEBS Lett. 261 (1990) 112-116.
6. E. J. Lyon, S. Shima, R. Boecher, R. K. Thauer, F.-W. Grevels, E. Bill, W. Roseboom, S. P. Albracht, J. Am. Chem. Soc. 126 (2004) 14239-14248.
7. E. J. Lyon, S. Shima, G. Buurman, S. Chowdhuri, A. Batschauer, K. Steinbach, R. K. Thauer, FEBS J. 271 (2004) 195-204.
8. S. Shima, D. Chen, T. Xu, M. D. Wodrich, T. Fujishiro, K. M. Schultz, J. Kahnt, K. Ataka, X. Hu, Nat. Chem. 7 (2015) 995-1002.
9. T. Xu, C.-J. M. Yin, M. D. Wodrich, S. Mazza, K. M. Schultz, R. Scopelliti, X. Hu, J. Am. Chem. Soc. 138 (2016) 3270-3273.
10. Y. Guo, H. Wang, Y. Xiao, S. Vogt, R. K. Thauer, S. Shima, P. I. Volkers, T. B. Rauchfuss, V. Pelmenschikov, D. A. Case, Inorg. Chem. 47 (2008) 3969-3977.
11. D. Chen, R. Scopelliti, X. Hu, Angew. Chem. Int. Ed. 49 (2010) 7512-7515.
12. C. K. Barik, R. Ganguly, Y. Li, W. K. Leong, Inorg. Chem. 57 (2018) 7113-7120.
13. C. K. Barik, R. Ganguly, Y. Li, C. Przybylski, M. Salmain, W. K. Leong, Inorg. Chem. 57 (2018**)** 12206-12212.
14. C. K. Barik, R. Ganguly, Y. Li, W. K. Leong, Eur. J. Inorg. Chem. 46 (2018) 4982-4986.
15. M. Cavicchioli, D. Bouyssi, J. Goré, G. Balme, Tetrahedron Lett. 37 (1996**)** 1429-1432.
16. S. M. Kupchan, R. W. Britton, M. F. Ziegler, C. J. Gilmore, R. J. Restivo, R. F. Bryan, J. Am. Chem. Soc. 95 (1973) 1335-1336.
17. R. A. Amos, J. A. Katzenellenbogen, J. Org. Chem. 43 (1978) 560-564.
18. M. Tori, Y. Shiotani, M. Tanaka, K. Nakashima, M. Sono, Tetrahedron Lett. 41 (2000) 1797-1799.
19. C. Mason, K. Edwards, R. Carlson, J. Pignatello, F. Gleason, J. Wood, Science 215 (1982) 400-402.
20. J. Drogosz, A. Janecka, Curr. Drug Targets 20 (2019) 444-452.
21. L. Chen, J.-P. Zhang, X. Liu, J. -J. Tang, P. Xiang, X.-M. Ma, Molecules 22 (2017) 1835.
22. G. Lyss, T. J. Schmidt, I. Merfort, H. L. Pahl, Biol. Chem. 378 (1997) 951-962.
23. D. L. Blithe, L. K. Nieman, R. P. Blye, P. Stratton, M. Passaro, Steroids 68 (2003) 1013-1017.
24. G. Scheid, W. Kuit, E. Ruijter, R. V. Orru, E. Henke, U. Bornscheuer, L. A. Wessjohann, Eur. J. Org. Chem. 2004 (2004) 1063-1074.
25. H.-L. Lu, Z.-W. Wu, S.-Y. Song, X.-D. Liao, Y. Zhu, Y.-S. Huang, Org. Process Res. Dev. 18 (2014) 431-436.
26. G. A. Krafft, J. A. Katzenellenbogen, J. Am. Chem. Soc. 103 (1981) 5459-5466.
27. T. Wakabayashi, Y. Ishii, K. Ishikawa, M. Hidai, Angew. Chem. Int. Ed. 35 (1996) 2123-2124.
28. J. Jeschke, C. Gäbler, M. Korb, T. Rüffer, H. Lang, Eur. J. Inorg. Chem. 2015 (2015) 2939-2947.
29. T. Mitsudo, Y. Hori, Y. Yamakawa, Y. Watanabe, J. Org. Chem. 52 (1987) 2230-2239.
30. K. Melis, D. De Vos, P. Jacobs, F. Verpoort, J. Organomet. Chem. 671 (2003) 131-136.
31. V. Cadierno, J. Francos, J. Gimeno, Organometallics 30 (2011) 852-862.
32. D. M. Chan, T. B. Marder, D. Milstein, N. J. Taylor, J. Am. Chem. Soc. 109 (1987) 6385-6388.

33. F. Neaţu, L. Proteşescu, M. Florea, V. I. Pârvulescu, C. M. Teodorescu, N. Apostol, P. Y. Toullec, V. Michelet, Green Chem. 12 (2010) 2145-2149.
34. J. Aleman, V. del Solar, C. Navarro-Ranninger, Chem. Comm. 46 (2010) 454-456.
35. L.-C. Lee, Y. Zhao, J. Am. Chem. Soc. 136 (2014) 5579-5582.
36. E. Tomás-Mendivil, P. Y. Toullec, J. Díez, S. Conejero, V. Michelet, V. Cadierno, Org. Lett. 14 (2012) 2520-2523.
37. M. Jiménez-Tenorio, M. C. Puerta, P. Valerga, F. J. Moreno-Dorado, F. M. Guerra, G. M. Massanet, Chem. Comm. 22 (2001) 2324-2325.
38. L.-C. Song, F.-Q. Hu, M.-M. Wang, Z.-J. Xie, K.-K. Xu, H.-B. Song, Dalton Trans. 43 (2014) 8062-8071.
39. R. D. Webster, A. M. Bond, T. Schmidt, J. Chem. Soc. Perk. T. 2. 7 (1995) 1365-1374.
40. J.-F. Capon, F. Gloaguen, P. Schollhammer, J. Talarmin, Coord. Chem. Rev. 249 (2005) 1664-1676.
41. G. A. Felton, C. A. Mebi, B. J. Petro, A. K. Vannucci, D. H. Evans, R. S. Glass, D. L. Lichtenberger, J. Organomet. Chem. 694 (2009) 2681-2699.
42. S. Canaguier, V. Fourmond, C. U. Perotto, J. Fize, J. Pécaut, M. Fontecave, M. J. Field, V. Artero, Chem. Comm. 49 (2013) 5004-5006.
43. P. D. Tran, J. Barber, Physical Chemistry Chemical Physics 14 (2012) 13772-13784.
44. J. C. Lansing, J. M. Camara, D. E. Gray, T. B. Rauchfuss, Organometallics 33 (2014) 5897-5906.